Far-Dissipation Range of Turbulence

Shiyi Chen and Gary Doolen
Theoretical Division and Center for Nonlinear Studies, Los Alamos National Laboratory, Los Alamos, New Mexico 87545

Jackson R. Herring
National Center for Atmospheric Research, Boulder, Colorado 80302

Robert H. Kraichnan
369 Montezuma 108, Santa Fe, New Mexico 87501

Steven A. Orszag
Program in Applied and Computational Mathematics, Princeton University, Princeton, New Jersey 08544

Zhen Su She
Mathematics Department, University of Arizona, Tucson, Arizona 85721
(Received 21 January 1993)

Navier-Stokes turbulence at low Reynolds number ($\mathcal{R}_\lambda \approx 15$) is studied by high-resolution computer simulation. The energy spectrum in the range $5k_d < k < 10k_d$ is well fitted by $k^\alpha \exp(-ck/k_d)$, where k_d is the Kolmogorov dissipation wave number, $\alpha \approx 3.3$ and $c \approx 7.1$. High-order spatial derivatives of the velocity field exhibit strong intermittency, associated with gentle spatial variation of large-scale structure rather than with sparse, intense small-scale structures. Analysis by the direct-interaction approximation, which ignores intermittency, gives $\alpha = 3$, $c \approx 11$.

PACS numbers: 47.27.Gs

The smallest scales of incompressible, isotropic Navier-Stokes turbulence are associated with the far-dissipation range of wave numbers $k \gg k_d$, where $k_d = \epsilon^{1/4}\nu^{-3/4}$ is the Kolmogorov dissipation wave number, ϵ is the rate of dissipation of hydrodynamic kinetic energy per unit mass, and ν is kinematic viscosity. Most of the dissipation takes place at $k < k_d$. The wave numbers $k \gg k_d$ have attracted attention for a number of years. There has been controversy concerning the asymptotic form of the energy spectrum as $k \to \infty$. The smallest scales are of further interest because they display strong intermittency even at Reynolds numbers so low that there is no basis for a fractal cascade.

It is reasonable to assume that the wave numbers $k \gg k_d$ represent spectral tails of flow structures of spatial scale $\geq 1/k_d$. An analogy is the exponential spectral tail of a shock that obeys the Burgers' equation. There are other possibilities. One is that very-high-wave-number excitation comes mostly from exceptionally strongly strained regions that give rise to observed exponential-like skirts of the probability distribution function (PDF) of vorticity.

A number of authors have discussed kinetic energy spectra for $k \gg k_d$ of the form

$$E(k) \propto f(k/k_d)\exp[-c(k/k_d)^n], \tag{1}$$

where c is a constant, f is a weak function of k/k_d, and $1 \leq n \leq 2$ [1–9]. The direct interaction approximation (DIA), a perturbative treatment, gives $n = 1$ and $f \propto (k/k_d)^3$ [2]. Perturbation approximation can be justified for $k \gg k_d$ because the mode amplitudes are very nearly the linear response, under molecular viscosity, to quadratic forcing by modes of lower k [10]. The additional, unjustified assumption in the DIA analysis is that the statistics of all scales are nearly Gaussian.

Foias, Manley, and Sirovich [4] have shown that $n \geq 1$, under certain assumptions of smoothness of the velocity field in a finite box. The plausible effect of the intermittency observed in the far-dissipation range is to enhance mean nonlinear transfer and thereby raise the spectrum level above that predicted by DIA. These two facts together suggest that the DIA value $n = 1$ may be exact for a finite box while $n > 1$ is unlikely [3]. The particular form

$$E(k) \propto k^\alpha \exp(-ck/k_d) \tag{2}$$

seems consistent with a body of experimental and computer data [8,9].

Strong intermittency in the far-dissipation range at low Reynolds numbers was predicted some years ago on the basis of a simple physical argument [10]: $E(k)$ falls off steeply for $k \gg k_d$. Consequently, mild fluctuation, on spatial macroscales, of parameters like k_d in (1) yields spatial intermittency at scales $O(1/k)$ that increases without limit as $k/k_d \to \infty$.

An ongoing computation project has achieved resolutions up to 512^3 (wave-number range $1 \leq k \leq 256$) on a CM-200 computer at Los Alamos National Laboratory [11]. The direct numerical simulation (DNS) described in this paper was limited by arithmetic precision rather than its resolution of 256^3 (wave-number range $1 \leq k \leq 128$ in a cyclic cube of side 2π). A nominal steady state was

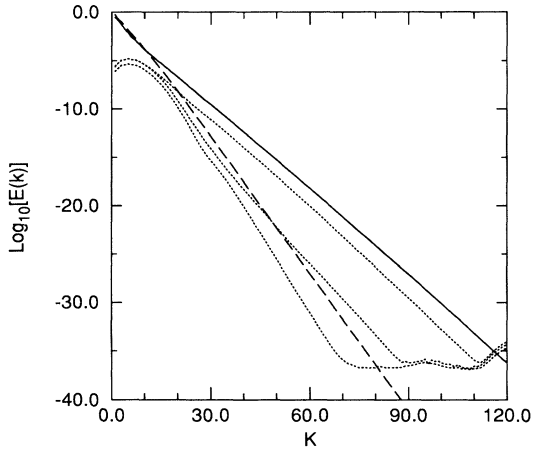

FIG. 1. Linear-log plot of $E(k)$ vs k. Solid line, DNS spectrum; dotted lines, subregional spectra with largest, median, and smallest values of $E(k = 60)$; dashed line, DIA spectrum.

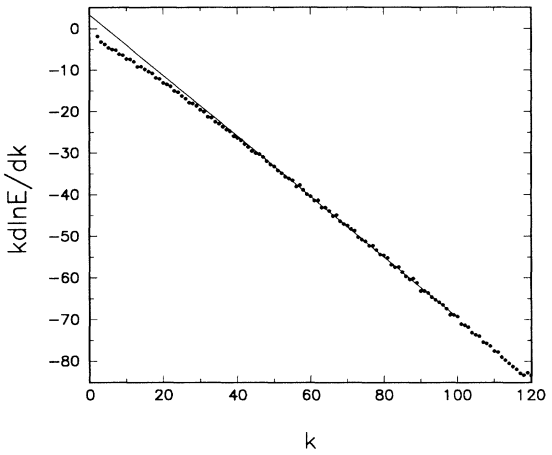

FIG. 2. The function $k\,d\ln E(k)/dk$ vs k for the DNS spectrum. The straight line is a least-squares fit to the data points for $50 \leq k \leq 100$.

maintained by forcing [11] that, at each time step, we reset the magnitude (but not the phase) of mode amplitudes for $k < 3$ to levels picked to give the desired value of the time-averaged Taylor microscale Reynolds number $\mathcal{R}_\lambda$. The simulation ran for approximately 40 box-size eddy-turnover times. The Taylor microscale λ for an isotropic turbulent flow is a length defined by $\lambda = (15\nu v_0^2/\epsilon)^{1/2}$, where v_0^2 is the mean-square velocity in any direction, and $\mathcal{R}_\lambda \equiv v_0\lambda/\nu$.

The solid line in Fig. 1 represents a time average of $E(k)$ for a run with $\nu = 0.026$, $\mathcal{R}_\lambda \approx 14.9$, $k_d \approx 9.65$. This $\mathcal{R}_\lambda$ is so low that there is no basis for a fractal cascade. Figure 2 shows $k\,d\ln E(k)/dk$ vs k for these data. If $E(k)$ has the form (2), the data fall on a straight line whose slope is $-c/k_d$ and whose intercept on the vertical axis is α. The straight line in Fig. 2 is a least-squares fit to the data over the range $50 \leq k \leq 100$, where the fit is excellent. Points $k < 50$ are excluded because the data there curve away from a straight line, and $k > 100$ is excluded because of truncation artifacts near $k = 128$.

The fit gives $c \approx 7.1$, $\alpha \approx 3.3$. Equation (2) seems well supported. The confidence level for α is hard to quantify because it is not certain that the wave-number range is long enough to give strictly asymptotic results. The value $n = 1$ in (1) does seem strongly favored.

A previous study [8] gave a negative value for α. The range used for fitting in [8] was $0.5k_d \leq k \leq 3k_d$, which is too low to give asymptotic behavior. An intercept $\alpha = 0$ corresponds to tangency at $k = 30 \approx 3k_d$ in Fig. 2 [12].

The dotted lines in Fig. 1 show the spectra in three subregions of the cyclic box, defined by the x-space filter $\exp[-|\mathbf{x}-\mathbf{x}_c|^2/(\pi/16)^2]$, where $\mathbf{x}_c$ is the subregion center. The nominal linear dimension of a subregion is thus $\pi/8$. In order to sufficiently reduce errors from chopping, the cyclic box is repeated in each direction to give a total of 3^3 replicas before the filtering. The filtered field is transformed to k space and subjected to solenoidal projection before the spectrum is computed.

We find that the distribution of spectral slopes over a set of 64 subregions, evenly spaced in the cyclic box, is consistent with the picture of intermittency [10] in which the parameters describing the spectral tail are slowly varying functions of spatial position. The three subregion spectra plotted in Fig. 1 are those with minimum, median, and maximum values of $E(k = 60)$. Note that the maximum and minimum values of $E(k = 60)$ differ by a factor of over 10^{10}, despite the small difference in slope.

Figure 3 shows PDFs of the differentiated velocity fields $(-\nabla^2)^m u_i$, averaged over the three components $i = 1, 2, 3$. Note the marked increase of intermittency

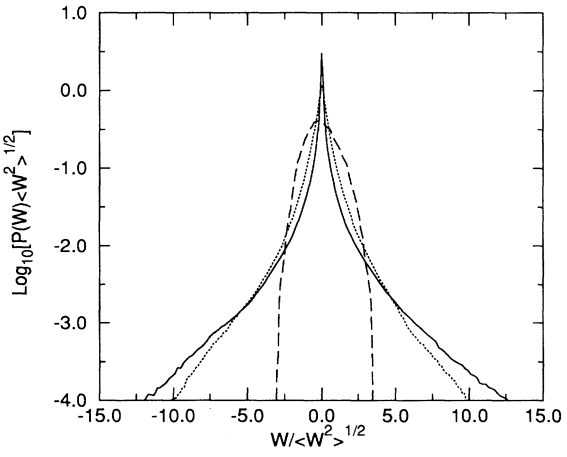

FIG. 3. PDF $P(w)$ of the field $w = (-\nabla^2)^m u_i$ for $m = 0$ (dashed), $m = 2$ (dotted), and $m = 4$ (solid), averaged over $i = 1, 2, 3$.

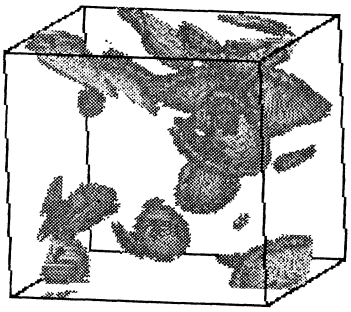

FIG. 4. Perspective view of the surface where $|\nabla^8 u_1|$ equals twice its root-mean-square value.

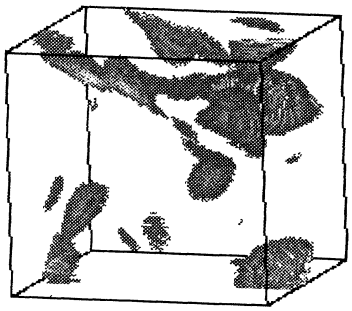

FIG. 5. Perspective view of the surface where the absolute value of the filtered field with spectral support centered at $k = 75$ equals twice its root-mean-square value.

with m. Figure 4 is a visualization of the field $\nabla^8 u_1$. The shaded surfaces are where the absolute value of field amplitude equals twice its root-mean-square (rms) value. The apparent three dimensionality of these regions (confirmed by interactive visualization) suggests intermittency that is associated with gentle spatial variation on principal dissipation scales rather than with exceptional regions that are strongly strained into thin sheets or tubes. The flatness $\langle(\nabla^8 u_1)^4\rangle/\langle(\nabla^8 u_1)^2\rangle^2$ is 57. This large value is associated mostly with the sharp peak of the PDF at zero amplitude, rather than with the broad skirts at large amplitude values. The latter represent probabilities too small to have much effect on low-order statistics.

The spectral support of the field $\nabla^8 u_1$ is effectively confined to the range $15 < k < 40$. A field with spectral support confined to $50 < k < 100$, the region where $E(k)$ is accurately proportional to $k^\alpha \exp(-ck/k_d)$, can be constructed by applying the filter $\exp[-(k-75)^2/200]$ to the wave-vector transform of $u_1(\mathbf{x})$ and transforming back to x space. Figure 5 shows the regions where the absolute value of the amplitude of this field exceeds twice its root-mean-square value. The field $\nabla^{24} u_1$ has approximately the same spectral support, but it is too noisy to give clean visualizations.

The similarity between Figs. 4 and 5 is striking. The regions of high intensity are in the same locations and have similar shape, but are smaller in Fig. 5. The similarities survive moderate changes in the choice of amplitude-to-rms ratio for visualization. This behavior suggests that the spectral support of the very small scales represents the spectral tail of larger structures. Similar behavior is exhibited by repeated differentiation of the velocity profile of a Burger's shock.

The small-scale structure portrayed in Fig. 5 is quite unlike the intense vortex tubes that characterize simulations at higher $\mathcal{R}_\lambda$ [13–15]. Nevertheless, Fig. 3 looks like plots of PDFs of velocity derivatives at higher $\mathcal{R}_\lambda$ [13–15]. Clearly, one-point PDFs provide insufficient information to infer the form of structures. It must be emphasized that $\mathcal{R}_\lambda$ in our simulation is too small to support an inertial-range cascade and fractal intermittency buildup that may be associated therewith [16]. We cannot assert from the present results that (2) remains valid at high $\mathcal{R}_\lambda$.

Integration of the DIA equations with the same forcing and viscosity as in the DNS yields the dashed line in Fig. 1. The DIA spectrum tail ($\alpha = 3$, $c \approx 11$) falls within the range of DNS subregion values, but below the median. There are two obvious causes for discrepancy between DIA and DNS. One is the depression of high-k energy transfer in DIA by sweeping effects in response functions [2]. At $k = 75$, the sweeping decorrelation frequency $v_0 k$ is about 30% of the viscous decay frequency νk^2. Two-point closures that are invariant to random Galilean transformation do not display the strong sweeping decorrelation at large k [17].

The second cause is the observed intermittency, which is not captured by DIA. Suppose that one emulates the set of subregion spectra by a finite-size ensemble of DIA solutions, each with a different forcing intensity. As $k \to \infty$, the mean spectrum over the ensemble is dominated by the ensemble member with the smallest value of c/k_d. Thus the effective value of c/k_d is decreased by the averaging, while the prefactor exponent $\alpha = 3$ is unchanged. The averaging over parameters may improve the fidelity of the DIA spectrum fit while crudely introducing strong intermittency at very small scales [10].

The spread in slope of the subregion spectra in Fig. 2 has an implication for the asymptotic spectrum form in an infinite box. Let the box size increase without limit while the forcing spectrum and filter width stay unchanged. Suppose that the spectrum ($k \to \infty$) in each finite subregion has exactly the form (2) where k_d is a function of $\mathbf{x}_c$. If any value of $k_d(\mathbf{x}_c)$, however large, occurs somewhere in the infinite box, then averaging over all space gives something slower than exponential decay of the spectrum as $k \to \infty$. Illustrative example: If the PDF of $k_d(\mathbf{x}_c)$ over the infinite box happens to be $\propto \exp(-k_d^2/k_e^2)$, as $k_d \to \infty$, where k_e is a constant parameter, averaging of (2) over this PDF gives an infinite-box spectrum $E(k) \propto \exp[-(2^{1/2}ck/k_e)^{2/3}]$ as $k \to \infty$, apart from an algebraic prefactor. The bound obtained

by Foias, Manley, and Sirovich [4] assumes a finite box.

The work reported here supports two principal conclusions about the dynamics of simulated isotropic turbulence at low $\mathcal{R}_\lambda$: First, the spectrum shape at $k \gg k_d$ can be accurately represented in the form (2); second, the high-k part of the velocity field is very intermittent despite the low value of $\mathcal{R}_\lambda$. The intermittency in our simulation is associated with gentle spatial variation of large-scale parameters, in contrast to the intermittency at higher $\mathcal{R}_\lambda$ linked to strongly localized intense vortex structures. Despite this contrast, the PDFs of high spatial derivatives of velocity look qualitatively the same at low and high values of $\mathcal{R}_\lambda$.

We thank Xiaowen Shan for help with the design of the computations and acknowledge valuable discussions with S. Kida, O. Manley, R. S. Rogallo, F. Waleffe, and Y. Zhou. D. W. Grunau and C. D. Hansen kindly produced the visualizations. This work was supported by the Department of Energy, the National Science Foundation, the Defense Advanced Research Projects Agency, and the Office of Naval Research. The computations were performed at the Advanced Computing Laboratory, Los Alamos National Laboratory and at the National Center for Atmospheric Research.

[1] A. A. Townsend, Proc. R. Soc. London A **208**, 534 (1951).
[2] R. H. Kraichnan, J. Fluid Mech. **5**, 497 (1959).
[3] S. A. Orszag, in *Fluid Dynamics*, edited by R. Balian and J.-L. Peube (Gordon and Breach, London, 1973), pp. 235–374.
[4] C. Foias, O. Manley, and L. Sirovich, Phys. Fluids A **2**, 464 (1990).
[5] L. M. Smith and W. C. Reynolds, Phys. Fluids A **3**, 992 (1991).
[6] O. Manley, Phys. Fluids A **4**, 1320 (1992).
[7] A. J. Domaradzki, Phys. Fluids A **4**, 2037 (1992).
[8] S. Kida, R. H. Kraichnan, R. S. Rogallo, F. Waleffe, and Y. Zhou (to be published).
[9] S. Grossmann and D. Lohse, Phys. Rev. A **46**, 903 (1992).
[10] R. H. Kraichnan, Phys. Fluids **10**, 2081 (1967).
[11] S. Chen, G. D. Doolen, R. H. Kraichnan, and Z. S. She, Phys. Fluids A **5**, 458 (1993).
[12] J. A. Domaradzki (private communication) has found that $\alpha > 0$ is favored by fits to several data sets in the range $k > 2k_d$.
[13] I. Hosokawa and K. Yamamoto, J. Phys. Soc. Jpn. **58**, 20 (1989).
[14] A. Vincent and M. Meneguzzi, J. Fluid Mech. **225**, 1 (1991).
[15] Z.-S. She, E. Jackson, and S. A. Orszag, Proc. R. Soc. London A **434**, 101 (1991).
[16] U. Frisch, Proc. R. Soc. London A **434**, 89 (1991).
[17] R. H. Kraichnan, Phys. Fluids **9**, 1728 (1966).